Structure of As-Se glasses by neutron diffraction with isotope substitution

Annalisa Polidori,[1,2] Anita Zeidler,[1] and Philip S. Salmon[1,*]

[1] *Department of Physics, University of Bath, Bath, BA2 7AY, UK*
[2] *Institut Laue Langevin, 71 Avenue des Martyrs, 38042 Grenoble Cedex 9, France*

(Dated: September 17, 2020)

The method of neutron diffraction with selenium isotope substitution is used to measure the structure of glassy $As_{0.30}Se_{0.70}$, $As_{0.35}Se_{0.65}$ and $As_{0.40}Se_{0.60}$. The method delivers three difference functions for each sample in which either the As-As, As-Se or Se-Se correlations are eliminated. The measured coordination numbers are consistent with the "8-N" rule and show that the $As_{0.30}Se_{0.70}$ network is chemically ordered, a composition near to which there is a minimum in the fragility index and a boundary to the intermediate phase. Chemical ordering in glassy $As_{0.35}Se_{0.65}$ and $As_{0.40}Se_{0.60}$ is, however, broken by the appearance of As-As bonds, the fraction of which increases with the arsenic content of the glass. For the $As_{0.40}Se_{0.60}$ material, a substantial fraction of As-As and Se-Se defect pairs (∼11%) is frozen into the network structure on glass formation.

I. INTRODUCTION

Chalcogenide glasses represent an important class of infrared transmitting materials with network structures and associated properties that can be tuned continuously by altering the chemical composition [1–3]. Here, the As-Se system is a prototype for which the "8-N" rule [4] predicts network structures based on threefold coordinated As and twofold coordinated Se atoms, where N is the number of valence electrons for a given chemical species. The glass structure therefore provides a contrast to the Ge-Se system where the network topology is based on fourfold coordinated Ge and twofold coordinated Se atoms. For all of these glasses, it is desirable to prepare realistic models of their atomic structures in a first step to predicting the material properties. Here, it is important to know the valency of the atomic species forming the network as well as the extent to which chemical ordering is preferred. For example, in the case of glassy $As_{0.40}Se_{0.60}$ and $Ge_{1/3}Se_{2/3}$ it is possible to construct networks in which all bonds are heteropolar, but this ideal of a chemically ordered network can be broken by the occurrence of homopolar bonds [5–8].

Constraint counting or rigidity theory is often used to provide an account of network properties. In the mean-field approach [9, 10], there is a transition from an elastically floppy under-constrained network to a stressed-rigid over-constrained network when the mean number of Lagrangian bonding constraints per atom is equal to three, the number of degrees of freedom per atom in three dimensions. If all bond-stretching and bond-bending constraints are intact and there are no dangling bonds, the transition between phases will occur when the mean coordination number equals 2.4. In the As-Se system, this coordination number corresponds to the composition $As_{0.40}Se_{0.60}$ where the atomic fraction of arsenic c_{As} = 0.40. The composition dependence of the density [11–13], glass transition temperature T_g [11–14], dielectric constant [11], elastic moduli [11, 12], activation energy for viscous flow [15] and fragility index [15, 16] all show a maximum at $c_{As} = 0.40$, where there is also a minimum in the Poisson ratio [12].

In comparison, if the network can self-organize during glass-formation to include atomic configurations that minimize over-constrained regions, then two transitions can occur such that the floppy and stressed-rigid phases are separated by a composition range known as the intermediate phase [17]. Intermediate phase compositions form networks that are isostatically rigid but stress free. The existence of an intermediate phase has been inferred from temperature-modulated differential scanning calorimetry (TMDSC) experiments in which the non-reversible enthalpy ΔH_{nr} takes a minimal value for a finite range of compositions [18]. For the As-Se system, this composition range is reported as $0.29(1) < c_{As} < 0.37(1)$ [19] or $0.27 < c_{As} < 0.37$ [16]. It does not therefore include the mean field expectation ($c_{As} = 0.40$), unlike systems such as Ge-Se [20–22]. This shift in composition may originate from a breakdown of the "8-N" rule, and the appearance of fourfold coordinated As atoms in quasi-tetrahedral Se=$AsSe_{3/2}$ units has been proposed [19, 23]. Indeed, a substantial breakdown of the "8-N" rule is reported for structural models of As-Se glasses that were obtained by combining x-ray anomalous scattering (AXS) experiments with the reverse Monte Carlo (RMC) method [24, 25]. A large breakdown of the rule is not, however, reported from first-principles molecular dynamics (FPMD) simulations [23, 24, 26, 27].

We have therefore been motivated to investigate the structure of As-Se glasses by using the method of neutron diffraction with selenium isotope substitution. The technique simplifies the complexity of correlations associated with a single diffraction pattern by enabling the formation of three difference functions for each sample in which either the As-As, As-Se or Se-Se correlations are eliminated. The objective is to provide an independent experimental test of the structural models that have been proposed, and to examine the extent to which the networks are chemically ordered. The focus of attention is on the compositions with c_{As} = 0.30, 0.35 and 0.40.

* Corresponding author: p.s.salmon@bath.ac.uk

The paper is organized as follows. The neutron diffraction theory is outlined in section II and the experimental methods are described in section III. The results are presented in section IV and are discussed in section V by reference to previous investigations on the structure of As-Se glasses. Conclusions are drawn in section VI.

II. THEORY

In a neutron diffraction experiment of an As-Se glass the total structure factor [28]

$$F(k) = \sum_{\alpha}\sum_{\beta} c_\alpha c_\beta b_\alpha b_\beta \left[S_{\alpha\beta}(k) - 1\right] \tag{1}$$

is measured, where k is the magnitude of the scattering vector, c_α and b_α are the atomic fraction and coherent neutron scattering length of chemical species α, and $S_{\alpha\beta}(k)$ is a Faber-Ziman partial structure factor. The corresponding real-space information is obtained by Fourier transformation and is represented by the total pair-distribution function

$$\begin{aligned} G(r) &= \frac{1}{2\pi^2\rho r}\int_0^\infty kF(k)\sin(kr)\,dk \\ &= \sum_{\alpha}\sum_{\beta} c_\alpha c_\beta b_\alpha b_\beta \left[g_{\alpha\beta}(r) - 1\right], \end{aligned} \tag{2}$$

where r is a distance in real space, ρ is the atomic number density, and $g_{\alpha\beta}(r)$ is a partial pair-distribution function. At r-values smaller than the distance of closest approach between the centres of two atoms $g_{\alpha\beta}(r \to 0) = 0$, so $G(r \to 0) \equiv G(0) = -\langle b\rangle^2$ where the mean scattering length $\langle b\rangle = c_{\rm As}b_{\rm As} + c_{\rm Se}b_{\rm Se}$. The coordination number obtained from $G(r)$ for the distance range $r_1 \le r \le r_2$ is given by

$$\begin{aligned} \bar{n} &= \frac{4\pi\rho}{|G(0)|}\int_{r_1}^{r_2}\left[G(r) - G(0)\right] r^2 dr \\ &= \frac{c_{\rm As}b_{\rm As}^2}{|G(0)|}\bar{n}_{\rm As}^{\rm As} + \frac{c_{\rm Se}b_{\rm Se}^2}{|G(0)|}\bar{n}_{\rm Se}^{\rm Se} + \frac{2c_{\rm As}b_{\rm As}b_{\rm Se}}{|G(0)|}\bar{n}_{\rm As}^{\rm Se} \end{aligned} \tag{3}$$

where, for this distance range, $\bar{n}_\alpha^\beta$ is the coordination number of chemical species β around an atom of chemical species α.

The complexity of correlations associated with a total structure factor can be simplified by using the difference function method. If ${}^{\rm nat}F(k)$ and ${}^{76}F(k)$ are the functions measured for two samples that are identical in every respect, except that one sample contains selenium of natural isotopic abundance ${}^{\rm nat}$Se and the other contains isotopically enriched ^{76}Se, then the As-As correlations can be eliminated by forming the difference function

$$\begin{aligned} \Delta F_{\rm Se}(k) &= {}^{76}F(k) - {}^{\rm nat}F(k) \\ &= a_1\left[S_{\rm AsSe}(k) - 1\right] + a_2\left[S_{\rm SeSe}(k) - 1\right] \end{aligned} \tag{4}$$

where $a_1 = 2c_{\rm As}c_{\rm Se}b_{\rm As}\left(b_{^{76}{\rm Se}} - b_{^{\rm nat}{\rm Se}}\right)$ and $a_2 = c_{\rm Se}^2\left(b_{^{76}{\rm Se}}^2 - b_{^{\rm nat}{\rm Se}}^2\right)$. Similarly, the As-Se correlations can be eliminated by forming the difference function

$$\begin{aligned} \Delta F_{\rm X}(k) &= \left(\frac{b_{^{\rm nat}{\rm Se}}}{b_{^{76}{\rm Se}}}\right){}^{76}F(k) - {}^{\rm nat}F(k) \\ &= b_1\left[S_{\rm AsAs}(k) - 1\right] + b_2\left[S_{\rm SeSe}(k) - 1\right] \end{aligned} \tag{5}$$

where $b_1 = c_{\rm As}^2 b_{\rm As}^2\left[\left(b_{^{\rm nat}{\rm Se}}/b_{^{76}{\rm Se}}\right) - 1\right]$ and $b_2 = c_{\rm Se}^2 b_{^{\rm nat}{\rm Se}}\left(b_{^{76}{\rm Se}} - b_{^{\rm nat}{\rm Se}}\right)$. The Se-Se correlations can be eliminated by forming the difference function

$$\begin{aligned} \Delta F_{\rm As}(k) &= {}^{\rm nat}F(k) - \left(\frac{b_{^{\rm nat}{\rm Se}}}{b_{^{76}{\rm Se}}}\right)^2{}^{76}F(k) \\ &= c_1\left[S_{\rm AsSe}(k) - 1\right] + c_2\left[S_{\rm AsAs}(k) - 1\right] \end{aligned} \tag{6}$$

where $c_1 = 2c_{\rm As}c_{\rm Se}b_{\rm As}b_{^{\rm nat}{\rm Se}}\left[1 - \left(b_{^{\rm nat}{\rm Se}}/b_{^{76}{\rm Se}}\right)\right]$ and $c_2 = c_{\rm As}^2 b_{\rm As}^2\left[1 - \left(b_{^{\rm nat}{\rm Se}}/b_{^{76}{\rm Se}}\right)^2\right]$.

The real-space functions $\Delta G_{\rm Se}(r)$, $\Delta G_{\rm X}(r)$ and $\Delta G_{\rm As}(r)$ corresponding to $\Delta F_{\rm Se}(k)$, $\Delta F_{\rm X}(k)$ and $\Delta F_{\rm As}(k)$, respectively, are obtained by Fourier transformation. For example,

$$\begin{aligned} \Delta G_{\rm Se}(r) &= \frac{1}{2\pi^2\rho r}\int_0^\infty k\Delta F_{\rm Se}(k)\sin(kr)\,dk \\ &= a_1\left[g_{\rm AsSe}(r) - 1\right] + a_2\left[g_{\rm SeSe}(r) - 1\right]. \end{aligned} \tag{7}$$

It follows that the low-r limits are given by $\Delta G_{\rm Se}(0) = -(a_1 + a_2)$, $\Delta G_{\rm X}(0) = -(b_1 + b_2)$ and $\Delta G_{\rm As}(0) = -(c_1 + c_2)$. In the case of $\Delta G_{\rm Se}(r)$, the coordination number for the range $r_1 \le r \le r_2$ is given by

$$\begin{aligned} \bar{n}_{\rm Se} &= \frac{4\pi\rho}{|\Delta G_{\rm Se}(0)|}\int_{r_1}^{r_2}\left[\Delta G_{\rm Se}(r) - \Delta G_{\rm Se}(0)\right] r^2 dr \\ &= \frac{(a_1/c_{\rm Se})}{|a_1 + a_2|}\bar{n}_{\rm As}^{\rm Se} + \frac{(a_2/c_{\rm Se})}{|a_1 + a_2|}\bar{n}_{\rm Se}^{\rm Se}. \end{aligned} \tag{8}$$

Similarly, the coordination number obtained from $\Delta G_{\rm X}(r)$ is given by

$$\bar{n}_{\rm X} = \frac{(b_1/c_{\rm As})}{|b_1 + b_2|}\bar{n}_{\rm As}^{\rm As} + \frac{(b_2/c_{\rm Se})}{|b_1 + b_2|}\bar{n}_{\rm Se}^{\rm Se}, \tag{9}$$

and the coordination number obtained from $\Delta G_{\rm As}(r)$ is given by

$$\bar{n}_{\rm As} = \frac{(c_1/c_{\rm Se})}{|c_1 + c_2|}\bar{n}_{\rm As}^{\rm Se} + \frac{(c_2/c_{\rm As})}{|c_1 + c_2|}\bar{n}_{\rm As}^{\rm As}. \tag{10}$$

In practice, a diffractometer can measure over only a finite k range up to a maximum value $k_{\rm max}$. In Eqs. (2) and (7), $F(k)$ or $\Delta F_{\rm Se}(k)$ is therefore multiplied by the step modification function $M(k) = 1$ for $k \le k_{\rm max}$, $M(k) = 0$ for $k > k_{\rm max}$, which can introduce Fourier transform artifacts if $k_{\rm max}$ is insufficiently large. The Lorch [29, 30] modification function $M(k) = \sin(\pi k/k_{\rm max})/(\pi k/k_{\rm max})$ for $k \le k_{\rm max}$, $M(k) = 0$ for $k > k_{\rm max}$ can be employed to obtain a smoother r-space function, but at the expense of broadened peaks.

III. EXPERIMENT

A. Sample preparation

The samples were prepared in silica ampoules of inner diameter 5 mm and wall thickness 1 mm. The ampoules were etched with a 48 wt% solution of hydrofluoric acid, rinsed with water then acetone, and dried under vacuum at 1073 K. The $As_{0.40}Se_{0.60}$ samples were prepared by loading an ampoule with As (99.99999+%, Alfa Aesar) and either ^{nat}Se (≥99.999%, Sigma Aldrich) or ^{76}Se (99.8% ^{76}Se, 0.2% ^{77}Se, Isoflex) inside a high-purity argon-filled glove box. The ampoule was isolated with a Young's tap and transferred to a vacuum line where it was evacuated to a pressure of $\approx 10^{-5}$ Torr and sealed. The ampoule was then placed in a furnace that rocked at a rate of 0.57 rpm with a maximum tilt angle of 30° to the horizontal. The temperature was increased at 1 K min^{-1} to the boiling point of Se at 958 K, dwelling for 4 h each at the melting point of Se (494 K) and the sublimation point of As (887 K). The highest temperature was maintained for 47 h before the rocking motion was stopped, the furnace was placed vertically, and the temperature was ramped down at 1 K min^{-1} to 673 K where it was maintained for 4 h. The ampoule was then dropped into an ice-water mixture. Each sample separated cleanly from its silica ampoule, which was opened in a high-purity argon-filled glove box where the glasses were subsequently handled. The mass of each sample was ∼1.8 g and the sample composition deduced from the mass was 0.4002(3) As: 0.5998(3) Se.

After the diffraction experiments were performed on the $As_{0.40}Se_{0.60}$ samples, the composition was adjusted to $As_{0.30}Se_{0.70}$ by adding As and either ^{nat}Se or ^{76}Se [31] and the glass-forming procedure was repeated. The mass of each sample was ∼2.6 g and the sample composition deduced from the mass was 0.3001(1) As: 0.6999(1) Se. After the diffraction experiments were performed on the $As_{0.30}Se_{0.70}$ samples, the composition was adjusted to $As_{0.35}Se_{0.65}$ by adding the required amount of As and the glass-forming procedure was repeated. The mass of each sample was ∼2.6 g and the sample composition deduced from the mass was 0.3501(1) As: 0.6499(1) Se.

The number density of each glass was measured using a pycnometer operated with helium gas. The values ρ = 0.03475(7) Å^{-3} for $As_{0.30}Se_{0.70}$, ρ = 0.0349(1) Å^{-3} for $As_{0.35}Se_{0.65}$ and ρ = 0.0354(1) Å^{-3} for $As_{0.40}Se_{0.60}$ were obtained. Characterization of a similarly prepared $As_{25}Se_{75}$ glass by energy dispersive x-ray spectroscopy and Raman spectroscopy found that the material is homogeneous on a sub-micron to centimeter length scale [32]. For glassy $As_{0.40}Se_{0.60}$, an onset value T_g = 458(1) K was obtained from the reversible heat flow measured in TMDSC experiments with a scan rate of 3 K min^{-1} and modulation rate of 1 K per 100 s, which compares to the value T_g = 458(9) K from [12].

TABLE I. Coefficients in Eqs. (4)–(10) for the neutron diffraction experiments on As-Se glasses. The coefficients are given in units of barn (1 barn = 10^{-28} m^2).

Coefficient	$As_{0.30}Se_{70}$	$As_{0.35}Se_{0.65}$	$As_{0.40}Se_{60}$
a_1	0.117(3)	0.126(3)	0.133(3)
a_2	0.418(8)	0.360(7)	0.306(6)
b_1	−0.0135(2)	−0.0184(3)	−0.0240(4)
b_2	0.165(4)	0.142(3)	0.121(3)
c_1	0.076(1)	0.083(1)	0.087(1)
c_2	0.0223(3)	0.0304(4)	0.0397(5)

B. Neutron diffraction experiments

Neutron diffraction experiments were performed at room temperature (≃298 K) on powdered glass samples held in a cylindrical vanadium container of inner diameter 0.48 mm and wall thickness 0.1 mm. The experiments on the $As_{0.40}Se_{0.60}$ samples employed the diffractometer D4c at the Institut Laue-Langevin [33] with an incident neutron wavelength of λ = 0.4991(1) Å. The diffractometer GEM at the ISIS pulsed neutron source [34] was also used to investigate the $As_{0.40}{}^{nat}Se_{0.60}$ sample. The experiments on the $As_{0.30}Se_{0.70}$ and $As_{0.35}Se_{0.65}$ samples employed GEM. Diffraction patterns were measured for each of the samples in its container, the empty container, the empty instrument, and a cylindrical vanadium rod of diameter 6.08 mm (D4c) or 6.04 mm (GEM) for normalization purposes. The relative counting times for the sample-in-container and empty container measurements were optimized in order to minimize the statistical error on the container-corrected intensity [35].

The D4c data analysis followed the procedure described in [36]. The GEM data analysis used the program Gudrun [37] with inelasticity corrections that were calculated according to [38]. Self-consistency checks were made to assess the reliability of the measured functions. For instance, it is necessary that (i) each of the measured total structure factors satisfies the sum-rule relation $\int_0^\infty dk\, k^2 F(k) = 2\pi^2 \rho G(0)$ that originates from Eq. (2); (ii) each of the measured $G(r)$ functions oscillates about its $G(0)$ limit at r-values smaller than the distance of closest approach between two atoms; and (iii) when these low-r oscillations in $G(r)$ are set to the calculated $G(0)$ limit, the back Fourier transform is in good overall agreement with the original total structure factor.

The scattering lengths taking into account the isotopic enrichment are b_{As} = 6.58(1) fm, $b_{^{nat}Se}$ = 7.970(9) fm and $b_{^{76}Se}$ = 12.19(10) fm [39]. An absorption cross-section of 115(23) barn for ^{76}Se at λ = 1.798 Å (cf. the value 85(7) barn from [39]) was deduced from a separate neutron diffraction experiment on isotopically enriched samples of glassy $GeSe_2$ that employed the GEM diffractometer. The values of the coefficients in Eqs. (4)–(10) are listed in Table I.

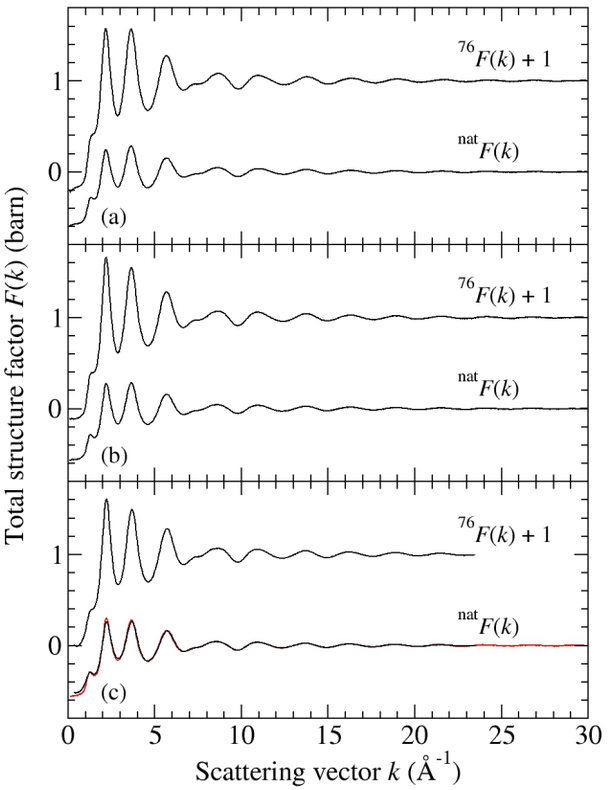

FIG. 1. Total structure factors $F(k)$ for as-prepared glassy (a) $As_{0.30}Se_{0.70}$, (b) $As_{0.35}Se_{0.65}$ and (c) $As_{0.40}Se_{0.60}$. The points with vertical error bars show the measured functions and the solid curves show spline fits. The error bars are smaller than the line thickness at most k values. The GEM data sets extend to $k_{max} = 40$ Å^{-1} but are shown over a smaller k-range for clarity of presentation. In (c) a comparison is made between the $^{nat}F(k)$ functions measured using D4c (black curve) versus GEM (red curve).

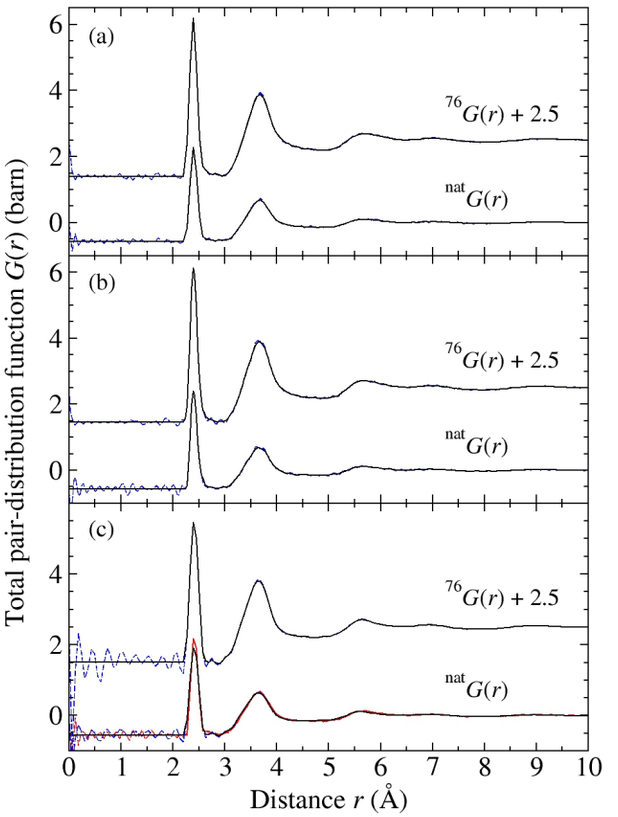

FIG. 2. Total pair-distribution functions $G(r)$ for glassy (a) $As_{0.30}Se_{0.70}$, (b) $As_{0.35}Se_{0.65}$ and (c) $As_{0.40}Se_{0.60}$. The broken curves show the Fourier transforms of the spline-fitted $F(k)$ functions shown in Fig. 1. The solid curves show the same functions after the low-r oscillations have been set to the $G(0)$ limit and the GEM data beyond the first peak have been smoothed by Fourier transforming $F(k)$ after the application of a Lorch modification function with $k_{max} = 40$ Å^{-1}. In (c) a comparison is made between the $^{nat}G(r)$ functions measured using D4c (black curves) versus GEM (red curves).

IV. RESULTS

The measured total structure factors for the As-Se glasses are shown in Fig. 1. For each glass there is a large contrast between the $^{nat}F(k)$ and $^{76}F(k)$ functions, and for each function there is a pre-peak or so-called first-sharp diffraction peak (FSDP) at $k_{FSDP} \sim 1.25$ Å^{-1} that is a signature of network ordering on an intermediate length scale [40]. In Fig. 1(c), a comparison is made between the $^{nat}F(k)$ functions measured using GEM versus D4c for $As_{0.40}Se_{0.60}$. There are small discrepancies that can be attributed largely to differences between the k-space resolution functions of the diffractometers, e.g., there is an asymmetrical broadening of the FSDP in the D4c data that originates from the "umbrella effect" [41].

The measured total pair-distribution functions are shown in Fig. 2 and the first peak positions and coordination numbers are listed in Table II. It is not possible to resolve the contributions to the first peak in the $G(r)$ functions from the different $g_{\alpha\beta}(r)$ functions on account of a similarity in the As-Se, As-As and Se-Se bond lengths. For example, the As-Se bond length is 2.389–2.453 Å in crystalline As_2Se_3 [42, 43] versus 2.365–2.418 Å in crystalline AsSe [44–46], the As-As bond length is 2.555–2.575 Å in crystalline AsSe [44–46] and the Se-Se bond length is 2.344(3) Å in glassy selenium [22]. In Fig. 2(c), a comparison is made between the $^{nat}G(r)$ functions measured using GEM versus D4c for $As_{0.40}Se_{0.60}$. The first peak at 2.413(1) Å (GEM) versus 2.414(1) Å (D4c) is broadened for the D4c data set on account of the smaller k-range that is accessible by D4c ($k_{max} = 23.45$ Å^{-1}) versus GEM ($k_{max} = 40$ Å^{-1}). The loss of r-space resolution is, however, small because the damped high-k oscillations die-out at $k \sim 30$ Å^{-1}. The first peak gives coordination numbers of $\bar{n} = 2.28(2)$ (GEM) versus $\bar{n} =$

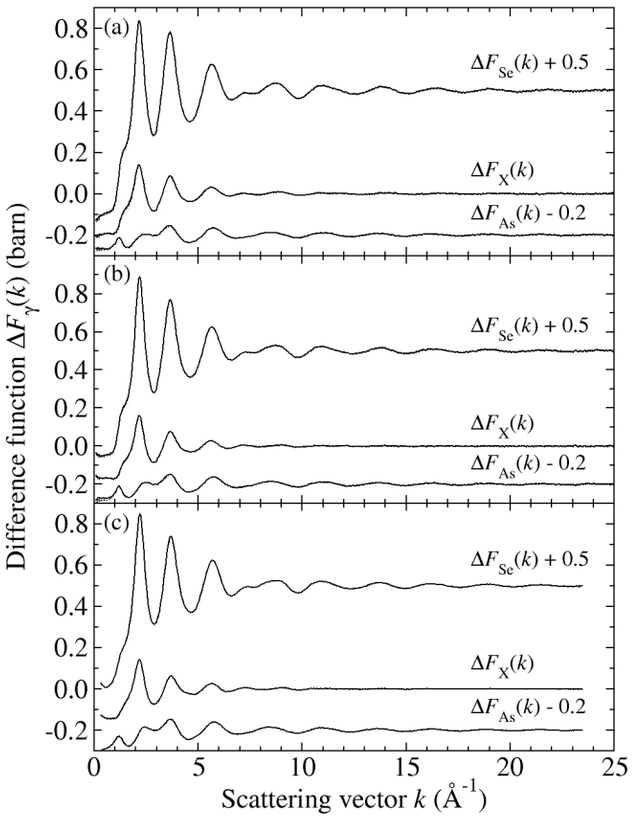

FIG. 3. Difference functions $\Delta F_\gamma(k)$ for glassy (a) $As_{0.30}Se_{0.70}$, (b) $As_{0.35}Se_{0.65}$ and (c) $As_{0.40}Se_{0.60}$. The points with vertical error bars show the measured functions and the solid curves show the back Fourier transforms of the $\Delta G_\gamma(r)$ functions given by the solid curves in Fig. 4. The error bars are smaller than the line thickness at most k values.

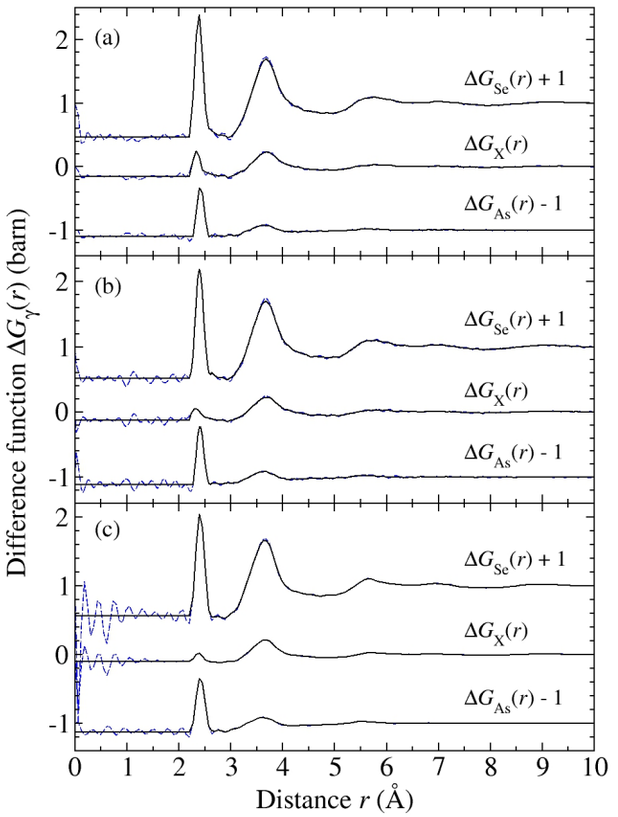

FIG. 4. Difference functions $\Delta G_\gamma(r)$ for glassy (a) $As_{0.30}Se_{0.70}$, (b) $As_{0.35}Se_{0.65}$ and (c) $As_{0.40}Se_{0.60}$. The broken curves show the Fourier transforms of the spline-fitted $\Delta F_\gamma(k)$ functions shown in Fig. 3. The solid curves show the same functions after the low-r oscillations have been set to the $\Delta G_\gamma(0)$ limit and the data beyond the first peak have been smoothed by Fourier transforming $\Delta F_\gamma(k)$ after the application of a Lorch modification function with k_{max} = 30 Å^{-1} (GEM) or 23.45 Å^{-1} (D4c).

2.33(2) (D4c), which are in accord with previous neutron diffraction work [47].

The measured difference functions $\Delta F_\gamma(k)$, where γ denotes Se, X or As, are shown in Fig. 3. The $\Delta F_{As}(k)$ function has a well-defined FSDP at $k_{FSDP} \sim 1.25$ Å^{-1} which, given the definition of this function [Eq. (6)], must originate from As-Se and/or As-As correlations. The corresponding r-space functions $\Delta G_\gamma(r)$ are shown in Fig. 4 where the GEM data sets were obtained by truncating the $\Delta F_\gamma(k)$ functions at k_{max} = 30 Å^{-1} because structural features are not perceptible at larger k values. The first peak positions and coordination numbers are listed in Table II. With increasing As content, there is little change to $\bar{n}_{Se}$ or $\bar{n}_{As}$ but a decrease in the value of $\bar{n}_X$. In the equation for $\bar{n}_X$, the coordination number $\bar{n}_{As}^{As}$ is given a negative weighting factor (Table I), so a decrease in $\bar{n}_X$ with increasing arsenic content is consistent with a decrease in $\bar{n}_{Se}^{Se}$ that is accompanied by an increase in $\bar{n}_{As}^{As}$.

V. DISCUSSION

A. Network models

The structure of glasses in the As-Se system has previously been investigated by FPMD [23, 24, 26, 27] and the AXS-RMC method where, in the modeling procedure, $\bar{n}_{Se}^{Se}$ was set to the value obtained from FPMD simulations [24, 25]. The bond lengths and coordination numbers obtained from these studies are compared in Table III. The partial structure factors and partial pair-distribution functions were used to construct the difference functions $\Delta F_\gamma(k)$ and $\Delta G_\gamma(r)$, respectively, for comparison with the neutron diffraction results (Figs. 5 and 6). Each technique gives $\Delta F_\gamma(k)$ functions that have the same shape, but there are important differences in detail that manifest themselves in r space. For example, relative to the neutron diffraction results, the first peak in the $\Delta G_{Se}(r)$

TABLE II. First peak positions $\bar{r}_1$ and coordination numbers obtained from the neutron diffraction work. $\bar{n}$ was obtained from $G(r)$ and $\bar{n}_\gamma$ was obtained from $\Delta G_\gamma(r)$ by integrating over the first peak in the measured r-space function.

	$As_{0.30}Se_{70}$		$As_{0.35}Se_{0.65}$		$As_{0.40}Se_{60}$	
Function	$\bar{r}_1$	$\bar{n}$ or $\bar{n}_\gamma$	$\bar{r}_1$	$\bar{n}$ or $\bar{n}_\gamma$	$\bar{r}_1$	$\bar{n}$ or $\bar{n}_\gamma$
$^{nat}G(r)$	2.398(1)	2.20(2)	2.400(1)	2.23(2)	2.414(1)	2.33(2)
$^{76}G(r)$	2.392(1)	2.01(2)	2.401(1)	1.97(2)	2.407(1)	2.01(2)
$\Delta G_{Se}(r)$	2.383(1)	1.76(2)	2.415(1)	1.75(4)	2.405(1)	1.71(2)
$\Delta G_X(r)$	2.338(1)	1.09(2)	2.349(10)	0.82(4)	2.384(1)	0.51(2)
$\Delta G_{As}(r)$	2.414(3)	3.30(4)	2.428(5)	3.44(4)	2.412(1)	3.27(2)

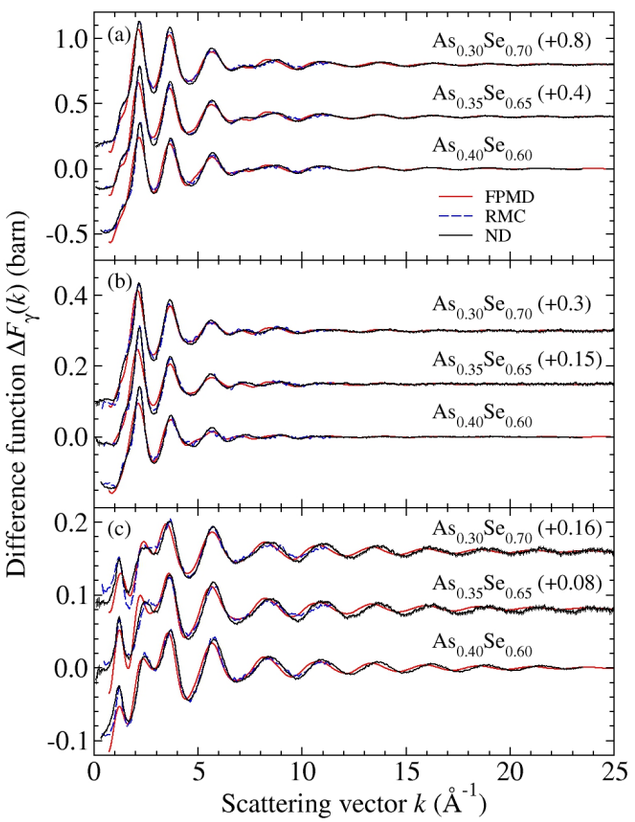

FIG. 5. Comparison between the difference functions (a) $\Delta F_{Se}(k)$, (b) $\Delta F_X(k)$ and (c) $\Delta F_{As}(k)$ obtained from FPMD [23] (solid red curves), AXS-RMC [25] (broken blue curves) and neutron diffraction (solid black curves). In the AXS-RMC work, the difference functions do not extend beyond $k_{max} = 11.4$ Å^{-1}, and the curves labelled $As_{0.30}Se_{0.70}$ and $As_{0.35}Se_{0.66}$ correspond to actual compositions of $As_{0.29}Se_{0.71}$ and $As_{0.33}Se_{0.67}$, respectively. Several of the curves have been offset vertically for clarity of presentation and the magnitude of the offset is indicated in parenthesis.

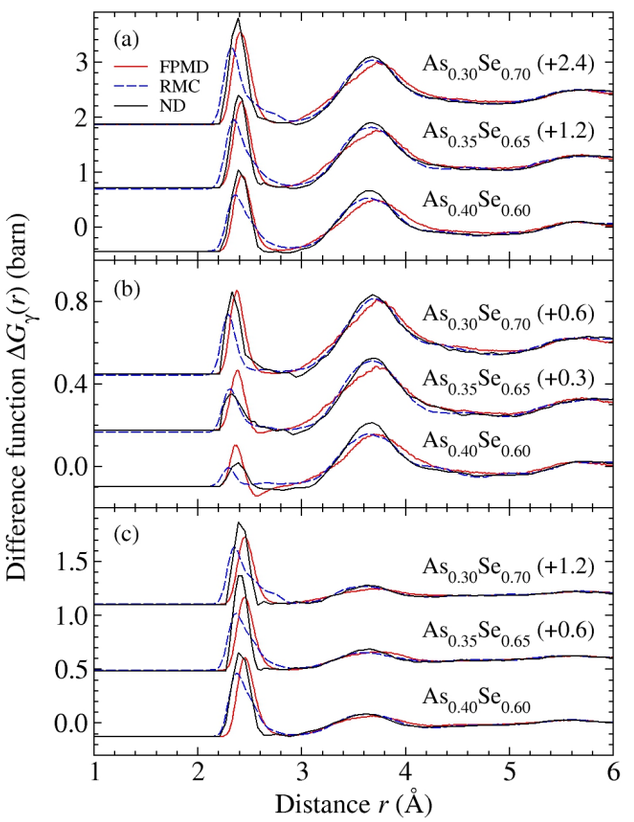

FIG. 6. Comparison between the difference functions (a) $\Delta G_{Se}(r)$, (b) $\Delta G_X(r)$ and (c) $\Delta G_{As}(r)$ obtained from FPMD [23] (solid red curves), AXS-RMC [25] (broken blue curves) and neutron diffraction (solid black curves). In the AXS-RMC work, the curves labelled $As_{0.30}Se_{0.70}$ and $As_{0.35}Se_{0.66}$ correspond to actual compositions of $As_{0.29}Se_{0.71}$ and $As_{0.33}Se_{0.67}$, respectively. Several of the curves have been offset vertically for clarity of presentation and the magnitude of the offset is indicated in parenthesis.

and $\Delta G_{As}(r)$ functions is shifted systematically towards a smaller r-value for the AXS-RMC results versus a larger r-value for the FPMD results. Relative to the neutron diffraction and FPMD results, the first peak in the AXS-RMC $\Delta G_{Se}(r)$ and $\Delta G_{As}(r)$ functions is also broadened asymmetrically. The coordination numbers are discussed in Section V B.

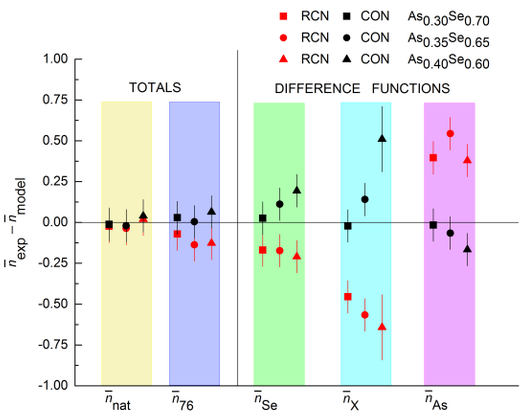

FIG. 7. Differences between the measured coordination numbers $\bar{n}$ or $\bar{n}_\gamma$ and those calculated using the CON (black markers) and RCN (red markers) models for glassy $As_{0.30}Se_{0.70}$ (squares), $As_{0.35}Se_{0.65}$ (circles) and $As_{0.40}Se_{0.60}$ (triangles). The $\bar{n}$ values for the samples containing $^{\rm nat}$Se and ^{76}Se are denoted by $\bar{n}_{\rm nat}$ and $\bar{n}_{76}$, respectively, and are highlighted in yellow and blue, respectively. The $\bar{n}_{\rm Se}$, $\bar{n}_{\rm X}$ and $\bar{n}_{\rm As}$ values are highlighted in green, cyan and magenta, respectively.

B. Chemical ordering and the "8-N" rule

Within the framework of the "8-N" rule, there are two contrasting models for the chemical ordering in glassy As-Se networks where arsenic and selenium have $Z_{\rm As} = 3$ and $Z_{\rm Se} = 2$ nearest-neighbor atoms, respectively. In the chemically ordered network (CON) model [48] there is a preference for heteropolar bonds. Homopolar bonds are absent at the composition where the number of As-Se bonds is equal to the number of Se-As bonds, i.e., when $c_{\rm As}Z_{\rm As} = c_{\rm Se}Z_{\rm Se}$ which corresponds to $c_{\rm As} = 0.40$. For Se-rich compositions ($c_{\rm As} < 0.40$), only As-Se and Se-Se bonds are allowed and the coordination numbers are $\bar{n}^{\rm Se}_{\rm As} = Z_{\rm As}$, $\bar{n}^{\rm Se}_{\rm Se} = Z_{\rm Se} - (c_{\rm As}/c_{\rm Se})\,Z_{\rm As}$ and $\bar{n}^{\rm As}_{\rm As} = 0$. For As-rich compositions ($c_{\rm As} > 0.40$), only As-Se and As-As bonds are allowed and the coordination numbers are $\bar{n}^{\rm As}_{\rm Se} = Z_{\rm Se}$ corresponding to $\bar{n}^{\rm Se}_{\rm As} = (c_{\rm Se}/c_{\rm As})\,Z_{\rm Se}$, $\bar{n}^{\rm Se}_{\rm Se} = 0$ and $\bar{n}^{\rm As}_{\rm As} = Z_{\rm As} - (c_{\rm Se}/c_{\rm As})\,Z_{\rm Se}$. By contrast, in the random covalent network (RCN) model [49], the distribution of bonds is purely statistical. The coordination numbers across the composition range are given by $\bar{n}^{\rm Se}_{\rm As} = c_{\rm Se}Z_{\rm Se}Z_{\rm Se}/2Z$, $\bar{n}^{\rm Se}_{\rm Se} = c_{\rm Se}Z^2_{\rm Se}/2Z$ and $\bar{n}^{\rm As}_{\rm As} = c_{\rm As}Z^2_{\rm As}/2Z$ where $Z = (c_{\rm As}Z_{\rm As} + c_{\rm Se}Z_{\rm Se})/2$ is the total number of bonds per atom.

The coordination numbers $\bar{n}_\gamma$ were calculated using the predictions of the CON and RCN models and a comparison with the measured values is given in Fig. 7. The results for $As_{0.30}Se_{0.70}$ show a chemically ordered network. The results for $As_{0.35}Se_{0.65}$ and $As_{0.40}Se_{0.60}$ show, however, discrepancies with the CON model that point to broken chemical ordering, but not to the extent given by the RCN model.

In order to find the coordination numbers $\bar{n}^\beta_\alpha$ that are consistent with the neutron diffraction results, the sum $\mathcal{S} = \sum_\gamma \left(\bar{n}^{\rm calc}_\gamma - \bar{n}^{\rm exp}_\gamma\right)^2$ was minimized with respect to the $\bar{n}^\beta_\alpha$ values, subject to the constraints that $Z_{\rm As} = 3$ and $Z_{\rm Se} = 2$, where "exp" refers to the measured value of $\bar{n}_\gamma$ and "calc" refers to the value of $\bar{n}_\gamma$ calculated from Eq. (8), (9) or (10). For the $c_{\rm As} = 0.30$ glass, the fitted coordination numbers (Table IV) are, within the experimental error, equal to those expected from the CON model which predicts $\bar{n}^{\rm As}_{\rm As} = 0$, $\bar{n}^{\rm Se}_{\rm As} = 3.0$ and $\bar{n}^{\rm Se}_{\rm Se} = 0.71$. The As-As coordination number then grows with the arsenic content of the glass. The total number of As-As bonds is given by $N_{\rm As-As} = N_{\rm As}\bar{n}^{\rm As}_{\rm As}/2$, where $N_{\rm As}$ is the total number of arsenic atoms in the glass and the factor of two is introduced to avoid double counting. It follows that $\bar{n}^{\rm As}_{\rm As} = 2N_{\rm As-As}/N_{\rm As}$, i.e., the measured $\bar{n}^{\rm As}_{\rm As}$ values show that the number of As-As bonds per arsenic atom increases with the arsenic content of the glass for $c_{\rm As} > 0.30$. Similarly, the measured $\bar{n}^{\rm Se}_{\rm Se}$ values show a decrease in the number of Se-Se bonds per selenium atom with increasing arsenic content.

In Table III, the coordination numbers obtained from $\mathcal{S}$ minimization are compared to the values obtained from other techniques. The constraint $Z_{\rm Se} = 2$ is in agreement with the predictions of the FPMD models, although the arsenic coordination numbers obtained from these simulations are 0.3–2.3% higher than the constraint $Z_{\rm As} = 3$ [23, 24, 26, 27]. The AXS-RMC models show, however, a substantial breakdown of the "8-N" rule associated with the arsenic atoms, delivering coordination numbers that are 8.7–23% larger than $Z_{\rm As} = 3$ [24, 25].

In order to investigate the compatibility of this scenario with the neutron diffraction results, the data sets were reanalysed by minimizing $\mathcal{S}$ subject to the constraint that $Z_{\rm As}$ and $Z_{\rm Se}$ take values that are consistent with the AXS-RMC models [24, 25]. Here, the values for the $c_{\rm As} = 0.30$ and $c_{\rm As} = 0.35$ compositions were obtained from the AXS-RMC results by linear interpolation. At all compositions, the revised fits give a substantial increase in the fraction of homopolar bonds and decrease in the fraction of heteropolar bonds (Table IV), leading to $\bar{n}^\beta_\alpha$ values that are substantially different to those obtained from the AXS-RMC models (Table III). The neutron diffraction results do not therefore support the AXS-RMC models for the As-Se glass structures.

Table III lists the coordination numbers obtained from ^{77}Se nuclear magnetic resonance (NMR) spectroscopy experiments on As-Se glasses annealed near to $T_{\rm g}$ [50, 51] and x-ray photoelectron spectroscopy (XPS) experiments on As-Se glasses that had been prepared by slow cooling, annealed near to $T_{\rm g}$ and aged at room temperature for 2–22 years [52, 53]. Deviations in the range from zero to ∼10% are found between the measured $\bar{n}^{\rm Se}_{\rm As}$ and $\bar{n}^{\rm Se}_{\rm Se}$ values and those expected from the CON model. It is difficult to assess the significance of these results because errors are seldom quoted. Table III also lists the coordination numbers obtained from ^{77}Se NMR spectroscopy experiments on Ge-doped As-Se glasses an-

TABLE III. Bond lengths and coordination numbers for As-Se glasses from (i) AXS-RMC models [24, 25], (ii) FPMD simulations and (iii) the present neutron diffraction (ND) work where the $\bar{n}_\alpha^\beta$ values were obtained by minimizing $\mathcal{S}$. Also listed are the coordination numbers found from ^{77}Se NMR experiments on As-Se [50, 51] or Ge-doped As-Se glasses [13] and XPS experiments on aged As-Se glasses [52, 53]. The total coordination numbers for As and Se are given by $Z_{\rm As} = \bar{n}_{\rm As}^{\rm As} + \bar{n}_{\rm As}^{\rm Se}$ and $Z_{\rm Se} = \bar{n}_{\rm Se}^{\rm Se} + \bar{n}_{\rm Se}^{\rm As}$, respectively. The CON model for glassy As-Se gives $\bar{n}_{\rm As}^{\rm Se} = 3$ and the listed $\bar{n}_{\rm Se}^{\rm Se}$ values.

$c_{\rm As}$	$\bar{r}_{\rm AsAs}$	$\bar{n}_{\rm As}^{\rm As}$	$\bar{r}_{\rm AsSe}$	$\bar{n}_{\rm As}^{\rm Se}$	$\bar{r}_{\rm SeSe}$	$\bar{n}_{\rm Se}^{\rm Se}$	$Z_{\rm As}$	$Z_{\rm Se}$	$\bar{n}_{\rm Se}^{\rm Se}$(CON)	Method
0.28	–	–	–	2.88	–	0.88	–	2.00	0.83	XPS
0.284	–	–	–	2.90(10)	–	0.82(3)	–	2.00	–	NMR[a]
0.29	2.41	0.12	2.35	3.57	2.29	0.54	3.69	2.00	0.77	AXS-RMC
0.30	2.57	0.07	2.47	2.94	2.39	0.74	3.01	2.00	0.71	FPMD [23]
0.30	–	0.01(5)	–	2.99(3)	–	0.72(2)	3	2		ND
0.30	–	–	–	2.94	–	0.74	–	2.00		XPS
0.33	2.45	0.24	2.37	3.05	2.31	0.50	3.29	2.00	0.52	AXS-RMC
0.34(1)	–	–	–	2.83	–	0.54	–	2.00	0.45	NMR
0.35	2.53	0.37	2.46	2.66	2.41	0.59	3.03	2.02	0.38	FPMD [23]
0.35	–	0.17(3)	–	2.83(4)	–	0.47(2)	3	2		ND
0.35	–	–	–	2.92	–	0.41	–	1.98		XPS
0.378	–	–	–	2.94(14)	–	0.13(1)	–	1.99	–	NMR[b]
0.40	2.41	0.73(1)	2.37(1)	2.53(1)	2.25	0.32(1)	3.26(2)	2.01(2)	0.00	AXS-RMC
0.40	2.58	0.70	2.48	2.31	2.42	0.45	3.01	1.99		FPMD [26]
0.40	2.55	0.65	2.45	2.40	2.37	0.42	3.05	2.02		FPMD [23]
0.40	2.55	0.53(2)	2.45(2)	2.54(1)	2.40	0.32(1)	3.07(3)	2.01(2)		FPMD [24]
0.40	–	0.63(2)	–	2.37(3)	–	0.42(2)	3	2		ND
0.40(2)	–	–	–	3.00	–	0.00	–	2.00		NMR
0.40	–	–	–	2.91	–	0.06	–	2.00		XPS

[a] Corresponds to $Ge_{1.6}As_{28.4}Se_{70}$; [b] Corresponds to $Ge_{2.2}As_{37.8}Se_{60}$

TABLE IV. Coordination numbers obtained by minimizing $\mathcal{S}$ subject to the constraint that the total As and Se coordination numbers satisfy either the "8-N" rule ($Z_{\rm As} = 3$ and $Z_{\rm Se} = 2$) or the results obtained from AXS-RMC models [25].

Glass	Fitted coordination number			Constraint		$\mathcal{S}$
	$\bar{n}_{\rm As}^{\rm As}$	$\bar{n}_{\rm As}^{\rm Se}$	$\bar{n}_{\rm Se}^{\rm Se}$	$Z_{\rm As}$	$Z_{\rm Se}$	
$As_{0.30}Se_{0.70}$	0.01(5)	2.99(3)	0.72(2)	3	2	0.0014
$As_{0.35}Se_{0.65}$	0.17(3)	2.83(4)	0.47(2)	3	2	0.0241
$As_{0.40}Se_{0.60}$	0.63(2)	2.37(3)	0.42(2)	3	2	0.0052
$As_{0.30}Se_{0.70}$	1.36(5)	2.23(5)	1.04(2)	3.59	2.00	0.0639
$As_{0.35}Se_{0.65}$	0.75(5)	2.53(5)	0.64(3)	3.28	2.00	0.0004
$As_{0.40}Se_{0.60}$	1.12(2)	2.14(2)	0.58(1)	3.26	2.01	0.0057

nealed at $T_{\rm g}$ [13]. Here, the CON predicts $\bar{n}_{\rm Se}^{\rm Se} = Z_{\rm Se} - (c_{\rm As}/c_{\rm Se})\, Z_{\rm As} - (c_{\rm Ge}/c_{\rm Se})\, Z_{\rm Ge} = 0.69$ for $Ge_{1.6}As_{28.4}Se_{70}$ ($Z_{\rm Ge} = 4$) and $\bar{n}_{\rm Se}^{\rm Se} = 0$ for the selenium poor composition $Ge_{2.2}As_{37.8}Se_{60}$ [54]. Hence, the Ge-doped glasses show broken chemical ordering with more Se-Se bonds than expected on the basis of the CON model. Other investigations using ^{77}Se NMR spectroscopy [55, 56], ^{75}As nuclear quadrupole resonance spectroscopy [57] and extended x-ray absorption fine structure (EXAFS) spectroscopy [58] do not report the presence of chemical disorder for glasses with compositions $c_{\rm As} \leq 0.40$, in accord with the CON model in which there are no As-As bonds and Se chains are cross-linked by $AsSe_{3/2}$ units. The variation in the reported results is linked to the sensitivity of the different experimental techniques, the model used to interpret the data, and a glass structure that is sensitive to its thermal history (Section V C).

C. Fraction of "wrong" bonds in glassy $As_{40}Se_{60}$

According to the CON model, homopolar bonds will be absent from the network structure of glassy $As_{40}Se_{60}$. These "wrong" bonds are, however, found in several investigations. The numbers of As-As and Se-Se bonds in the glass are given by $N_{\rm As-As} = N_{\rm As}\bar{n}_{\rm As}^{\rm As}/2 = c_{\rm As}N\bar{n}_{\rm As}^{\rm As}/2$ and $N_{\rm Se-Se} = N_{\rm Se}\bar{n}_{\rm Se}^{\rm Se}/2 = c_{\rm Se}N\bar{n}_{\rm Se}^{\rm Se}/2$, respectively, where $N_{\rm Se}$ is the number of selenium atoms and N is the total number of atoms. From these expressions and the coordination numbers measured by neutron diffraction (Table III), it follows that $N_{\rm As-As} = 0.126(6)N$ and $N_{\rm Se-Se} = 0.126(4)N$, i.e., the number of these bonds is

the same within the experimental error. The bonds appear therefore in pairs according to the reversible reaction

$$2\text{As}{-}\text{Se} \rightleftharpoons \text{As}{-}\text{As} + \text{Se}{-}\text{Se}. \quad (11)$$

From the law of mass action, the equilibrium constant for the reaction in Eq. (11) can be written in the form $N_\text{d}/N_\text{bond} \simeq \exp(-\Delta G/2\text{R}T_\text{g})$ where the number of defect pairs $N_\text{d} = N_{\text{As}-\text{As}} = N_{\text{Se}-\text{Se}}$, ΔG is the standard reaction Gibbs energy, and R is the molar gas constant [5, 6, 59]. By using As-Se, As-As and Se-Se bond enthalpies of 230, 200 and 225 kJ mol^{-1} [6], respectively, the value $\Delta G = 35$ kJ mol^{-1} is estimated and the fraction of defect pairs at $T_\text{g} = 456$ K is given by $N_\text{d}/N_\text{bond} = 0.010$. In comparison, As-Se, As-As and Se-Se bond energies of 227, 202 and 223 kJ mol^{-1} [60], respectively, give $\Delta G = 29$ kJ mol^{-1} and $N_\text{d}/N_\text{bond} = 0.022$. A comparable value $N_\text{d}/N_\text{bond} \simeq 0.005$ at T_g is obtained from a similar approach in which the difference in bond energies was estimated from the As and Se electronegativity difference [61]. In contrast, a significantly larger value of $N_\text{d}/N_\text{bond} = ZN_\text{d}/N = 0.105(4)$ is obtained from the neutron diffraction results, where the total number of bonds in the glass is given by $N_\text{bond} = ZN$ (Section V B).

The discrepancy between the measured and calculated N_d/N_bond values can be alleviated by using the quench temperature $T_\text{q} = 673$ K (Section III A) in place of T_g, which gives $N_\text{d}/N_\text{bond} \simeq \exp(-\Delta G/2\text{R}T_\text{q}) = 0.075$ for $\Delta G = 29$ kJ mol^{-1}. It is therefore possible that a large fraction of "wrong" bonds in the melt are frozen into the glass structure on rapid quenching. Indeed, ^{75}As nuclear quadrupole resonance experiments find that rapidly-drawn fibers of glassy $As_{40}Se_{60}$ show a measurable quantity of As-As homopolar bonds [62], and EXAFS and Raman spectroscopy experiments on evaporated films of $As_{40}Se_{60}$ show the presence of homopolar bonds and their removal by thermal annealing [63]. In the neutron diffraction work, the $As_{40}Se_{60}$ glass was fast-quenched, the material was unannealed, and $\bar{n}_\text{Se}^\text{Se} = 0.42(2)$ (Table III). By comparison, in the XPS work [52, 53], the $As_{40}Se_{60}$ glass was made by slow cooling, the material was annealed near T_g and aged at room temperature for 22 years, and $\bar{n}_\text{Se}^\text{Se} = 0.06$. These findings point towards the creation of "wrong" bonds by rapid quenching and their removal by thermal treatment. It would therefore seem prudent to use temperature-dependent constraint theory to provide an account of network properties in the As-Se system [64].

In the case of glassy $Ge_{1/3}Se_{2/3}$, the CON model also gives a network structure in which homopolar bonds are absent. Experiment shows, however, that homopolar bonds are present, and the fraction of Ge-Ge and Se-Se defect pairs obtained from the coordination numbers measured by neutron diffraction is given by $N_\text{d}/N_\text{bond} \simeq 0.04(2)$ [7, 59], which is in accord with the value $N_\text{d}/N_\text{bond} \simeq 0.042$ at T_g estimated from the law of mass action [5, 6]. For this material, neutron diffraction results do not show a large difference in the Ge-Ge and Se-Se coordination numbers between the glass and high-temperature liquid, i.e., the fraction of "wrong" bonds in the glass is similar to the melt [7, 8, 65]. This fraction is much smaller than indicated by the experimental and FPMD work on glassy $As_{40}Se_{60}$, so it appears that germanium atoms are less prone to forming homopolar bonds than arsenic atoms.

D. Glass structure and material properties

The composition dependence of a set of material properties, namely the density, glass transition temperature, dielectric constant, elastic moduli, activation energy for viscous flow, fragility index and Poisson ratio, all show an extremum at $c_\text{As} = 0.40$ (Section I). This composition coincides with the expectation from mean-field constraint counting theory for a change in the elastic properties of As-Se network structures. The network at this composition is not necessarily chemically ordered on account of the observation from several techniques of a large fraction of homopolar bonds. The analysis of Section V C indicates that the concentration of these "wrong" bonds is sensitive to the thermal history of the glass, pointing to the need for temperature dependent constraints in modeling the As-Se system using rigidity theory.

The same set of material properties show a continuous variation over the range of compositions $0.29(1) < c_\text{As} < 0.37(1)$ [19] or $0.27 < c_\text{As} < 0.37$ [16] reported for the intermediate phase. (The minimum in molar volume reported by Ravindren et al. [16] for the range $0.20 < c_\text{As} < 0.30$ is not found in other investigations [11, 12, 66].) Here, it should be noted that TMDSC experiments on As-Se glasses that were aged for 2–22 years did not find a minimum in ΔH_nr in the composition range reported for the intermediate phase [16, 19], but find $\Delta H_\text{nr} \simeq 0$ at the mean-field expectation $c_\text{As} = 0.40$ [53]. Notwithstanding, the fragility index of the melt shows a minimum at $c_\text{As} \simeq 0.25$–0.30 [15, 16, 66] and, for intermediate phase compositions, FPMD simulations find a maximum in the self-diffusion coefficients of the As and Se atoms and a minimum in the activation energy for diffusion of each of these atoms [23, 27]. The boundary of the intermediate phase at $c_\text{As} \sim 0.27$–0.29 may be associated with the formation of a chemically ordered network as found in the present neutron diffraction work on glassy $As_{0.30}Se_{0.70}$, a composition at which FPMD simulations show a minimum in the fraction of homopolar bonds [27]. There is no obvious structural signature of the other boundary reported for the intermediate phase at $c_\text{As} = 0.37(1)$.

For the Ge-Se system, a recent systematic investigation [22] did not find evidence of a structural origin for the intermediate phase, but the composition range does correspond to a maximum in the viscosity at the liquidus temperature and a minimum in the fragility index. It therefore appears that the origin of the intermediate phase in the Ge-Se and As-Se systems, as found from the behavior of ΔH_nr measured using TMDSC at tempera-

tures corresponding to the glass transition, is linked to the dynamical properties of these materials in the liquid state.

VI. CONCLUSIONS

The method of neutron diffraction with Se isotope substitution was used to measure the difference functions $\Delta F_\gamma(k)$ over a wide k-range, thus delivering $\Delta G_\gamma(r)$ functions with excellent r-space resolution. The measured coordination numbers are consistent with the "8-N" rule for both As and Se atoms. The $Z_{\rm Se} = 2$ value is in accord with FPMD simulations [23, 26, 27], which also find that $Z_{\rm As} = 3$ is exceeded by a small amount (0.3–2.3%). The results are incompatible with AXS-RMC models of As-Se glasses [24, 25] in which $Z_{\rm As} = 3$ is exceeded by 8.7–23%.

The neutron diffraction work indicates complete chemical ordering for glassy $As_{0.30}Se_{0.70}$, a composition near to which there is a minimum in the fragility index [15, 16, 66] and a boundary to the intermediate phase [16, 19]. There is no obvious structural signature of the other boundary reported for the intermediate phase at $c_{\rm As} = 0.37(1)$. The fraction of As-As bonds increases with the arsenic content of the glass for $c_{\rm As} > 0.30$. The chemical ordering is therefore broken for glassy $As_{0.35}Se_{0.65}$ and $As_{0.40}Se_{0.60}$, but not to the extent indicated by the RCN model. The broken chemical disorder is nonetheless substantial: For $As_{0.40}Se_{0.60}$, the fraction of As-As and Se-Se defect pairs frozen into the network structure on glass formation is $N_{\rm d}/N_{\rm bond} = 0.105(4)$.

ACKNOWLEDGMENTS

We thank Keiron Pizzey (Bath) for help with the sample preparation and D4c experiment, Henry Fischer (ILL) for help with the D4c experiment, and Alex Hannon (ISIS) for help with the GEM experiment. We also thank Shinya Hosokawa (Kumamoto) and Matthieu Micoulaut (Paris) for the provision of their data sets and Sabyasachi Sen (UC Davis) for useful discussions. The work in Bath was supported by the EPSRC (Grant No. EP/J009741/1). AP acknowledges funding and support from the Institut Laue Langevin (ILL) and University of Bath (Collaboration Agreement ILL-1353.1). AZ is supported by a Royal Society-EPSRC Dorothy Hodgkin Research Fellowship. We acknowledge use of the Engineering and Physical Sciences Research Council (EPSRC) funded National Chemical Database Service hosted by the Royal Society of Chemistry.

PSS and AZ designed the diffraction work and AZ prepared the samples. AP, PSS and HEF performed the diffraction experiments, and AP, AZ and PSS analyzed the data. PSS wrote the paper with input from co-authors.

Data access statement

The data sets created during this research are openly available from the University of Bath Research Data Archive at https://doi.org/10.15125/BATH-00902 [67].

[1] Z. U. Borisova, *Glassy Semiconductors* (Springer, New York, 1981).
[2] K. Tanaka and K. Shimakawa, *Amorphous Chalcogenide Semiconductors and Related Materials* (Springer, New York, 2011).
[3] J.-L. Adam and X. Zhang, eds., *Chalcogenide Glasses: Preparation, Properties and Applications*, Woodhead Publishing Series in Electronic and Optical Materials: Number 44 (Woodhead Publishing, Oxford, 2014).
[4] J. Robertson, Phys. Status Solidi A **213**, 1641 (2016).
[5] A. Feltz, in *Physics of Disordered Materials*, edited by D. Adler, H. Fritzsche, and S. R. Ovshinsky (Plenum, New York, 1985) pp. 203–213.
[6] A. Feltz, *Amorphous Inorganic Materials and Glasses* (VCH, Weinheim, 1993).
[7] I. Petri, P. S. Salmon, and H. E. Fischer, Phys. Rev. Lett. **84**, 2413 (2000).
[8] P. S. Salmon and I. Petri, J. Phys.: Condens. Matter **15**, S1509 (2003).
[9] J. C. Phillips, J. Non-Cryst. Solids **34**, 153 (1979).
[10] M. F. Thorpe, J. Non-Cryst. Solids **57**, 355 (1983).
[11] A. Feltz, H. Aust, and A. Blayer, J. Non-Cryst. Solids **55**, 179 (1983).
[12] G. Yang, B. Bureau, T. Rouxel, Y. Gueguen, O. Gulbiten, C. Roiland, E. Soignard, J. L. Yarger, J. Troles, J.-C. Sangleboeuf, and P. Lucas, Phys. Rev. B **82**, 195206 (2010).
[13] D. C. Kaseman, I. Hung, Z. Gan, B. Aitken, S. Currie, and S. Sen, J. Phys. Chem. B **118**, 2284 (2014).
[14] R. Blachnik and A. Hoppe, J. Non-Cryst. Solids **34**, 191 (1979).
[15] G. Yang, O. Gulbiten, Y. Gueguen, B. Bureau, J.-C. Sangleboeuf, C. Roiland, E. A. King, and P. Lucas, Phys. Rev. B **85**, 144107 (2012).
[16] S. Ravindren, K. Gunasekera, Z. Tucker, A. Diebold, P. Boolchand, and M. Micoulaut, J. Chem. Phys. **140**, 134501 (2014).
[17] M. F. Thorpe, D. J. Jacobs, M. V. Chubynsky, and J. C. Phillips, J. Non-Cryst. Solids **266-269**, 859 (2000).
[18] P. Boolchand, D. G. Georgiev, and B. Goodman, J. Optoelectron. Adv. Mater. **3**, 703 (2001).
[19] D. G. Georgiev, P. Boolchand, and M. Micoulaut, Phys. Rev. B **62**, R9228 (2000).
[20] X. Feng, W. J. Bresser, and P. Boolchand, Phys. Rev. Lett. **78**, 4422 (1997).
[21] S. Bhosle, K. Gunasekera, P. Boolchand, and M. Micoulaut, Int. J. Appl. Glass Sci. **3**, 205 (2012).

[22] A. Zeidler, P. S. Salmon, D. A. J. Whittaker, K. J. Pizzey, and A. C. Hannon, Front. Mater. **4**, 32 (2017).
[23] M. Bauchy, A. Kachmar, and M. Micoulaut, J. Chem. Phys. **141**, 194506 (2014).
[24] S. Hosokawa, A. Koura, J.-F. Bérar, W.-C. Pilgrim, S. Kohara, and F. Shimojo, Europhys. Lett. **102**, 66008 (2013).
[25] S. Hosokawa, W.-C. Pilgrim, J.-F. Bérar, and P. Boolchand, J. Non-Cryst. Solids **431**, 31 (2016).
[26] J. Li and D. A. Drabold, Phys. Rev. B **61**, 11998 (2000).
[27] M. Bauchy, M. Micoulaut, M. Boero, and C. Massobrio, Phys. Rev. Lett. **110**, 165501 (2013).
[28] H. E. Fischer, A. C. Barnes, and P. S. Salmon, Rep. Prog. Phys. **69**, 233 (2006).
[29] E. Lorch, J. Phys. C: Solid State Phys. **2**, 229 (1969).
[30] P. S. Salmon, J. Phys.: Condens. Matter **18**, 11443 (2006).
[31] The provision of additional isotopes enabled the preparation of larger glassy samples. Hence, both As and Se were added to adjust the $As_{0.40}Se_{0.60}$ composition to the $As_{0.30}Se_{0.70}$ composition.
[32] P. Lucas, G. J. Coleman, S. Sen, S. Cui, Y. Guimond, L. Calvez, C. Boussard-Pledel, B. Bureau, and J. Troles, J. Chem. Phys. **150**, 014505 (2019).
[33] H. E. Fischer, G. J. Cuello, P. Palleau, D. Feltin, A. C. Barnes, Y. S. Badyal, and J. M. Simonson, Appl. Phys. A **74**, S160 (2002).
[34] A. C. Hannon, Nucl. Instrum. Methods Phys. Res. A **551**, 88 (2005).
[35] P. S. Salmon, A. Zeidler, and H. E. Fischer, J. Appl. Cryst. **49**, 2249 (2016).
[36] P. S. Salmon, S. Xin, and H. E. Fischer, Phys. Rev. B **58**, 6115 (1998).
[37] S. E. McLain, D. T. Bowron, A. C. Hannon, and A. K. Soper, *Gudrun: A computer program developed for analysis of neutron diffraction data*, Tech. Rep. (ISIS Facility, Rutherford Appleton Laboratory, Chilton, Didcot, Oxon, United Kingdom OX11 0QX, 2006).
[38] M. A. Howe, R. L. McGreevy, and W. S. Howells, J. Phys.: Condens. Matter **1**, 3433 (1989).
[39] V. F. Sears, Neutron News **3**, 26 (1992).
[40] P. S. Salmon, Proc. R. Soc. Lond. A **445**, 351 (1994).
[41] P. S. Salmon, I. Petri, P. H. K. de Jong, P. Verkerk, H. E. Fischer, and W. S. Howells, J. Phys.: Condens. Matter **16**, 195 (2004).
[42] A. S. Kanishcheva, Y. N. Mikhailov, E. G. Zhokov, and T. G. Grevtseva, Izvestiya Akademii Nauk SSSR, Neorganicheskie Materialy **19**, 1744 (1983).
[43] A. C. Stergiou and P. J. Rentzeperis, Z. Kristallogr. **173**, 185 (1985).
[44] T. J. Bastow and H. J. Whitfield, J. Chem. Soc., Dalton Trans. , 1739 (1973).
[45] P. Goldstein and A. Paton, Acta Crystallogr. B **30**, 915 (1974).
[46] E. J. Smail and G. M. Sheldrick, Acta Crystallogr. B **29**, 2014 (1973).
[47] S. Xin, J. Liu, and P. S. Salmon, Phys. Rev. B **78**, 064207 (2008).
[48] R. M. White, J. Non-Cryst. Solids **16**, 387 (1974).
[49] K. S. Liang, A. Bienenstock, and C. W. Bates, Phys. Rev. B **10**, 1528 (1974).
[50] M. Deschamps, C. Roiland, B. Bureau, G.Yang, L. Le Pollèes, and D. Massiot, Solid State Nucl. Magnet. Res. **40**, 72 (2011).
[51] M. Deschamps, C. Genevois, S. Cui, C. Roiland, L. Le Pollès, E. Furet, D. Massiot, and B. Bureau, J. Phys. Chem. C **119**, 11852 (2015).
[52] R. Golovchak, A. Kovalskiy, A. C. Miller, H. Jain, and O. Shpotyuk, Phys. Rev. B **76**, 125208 (2007).
[53] R. Golovchak, H. Jain, O. Shpotyuk, A. Kozdras, A. Saiter, and J.-M. Saiter, Phys. Rev. B **78**, 014202 (2008).
[54] For the same Ge:As ratio of 1:17.1818, the network is chemically ordered with only As-Se and Ge-Se bonds at the composition $Ge_{2.1761}As_{37.3889}Se_{60.435}$.
[55] B. Bureau, J. Troles, M. Le Floch, F. Smektala, and J. Lucas, J. Non-Cryst. Solids **326–327**, 58 (2003).
[56] B. Bureau, J. Troles, M. Le Floch, F. Smektala, G. Silly, and J. Lucas, Solid State Sci. **5**, 219 (2003).
[57] E. Ahn, G. A. Williams, and P. C. Taylor, Phys. Rev. B **74**, 174206 (2006).
[58] V. Mastelaro, H. Dexpert, S. Benazeth, and R. Ollitrault-Fichet, J. Solid State Chem. **96**, 301 (1992).
[59] P. S. Salmon and A. Zeidler, in *Molecular Dynamics Simulations of Disordered Materials*, Springer Series in Materials Science 215, edited by C. Massobrio, J. Du, M. Bernasconi, and P. S. Salmon (Springer, Cham, Switzerland, 2015) Chap. 1, pp. 1–31.
[60] E. V. Shkol'nikov, Glass Phys. Chem. **11**, 40 (1985).
[61] D. Vanderbilt and J. D. Joannopoulos, Phys. Rev. B **23**, 2596 (1981).
[62] P. Hari, P. C. Taylor, W. A. King, and W. C. LaCourse, J. Non-Cryst. Solids **198–200**, 736 (1996).
[63] R. J. Nemanich, G. A. N. Connell, T. M. Hayes, and R. A. Street, Phys. Rev. B **18**, 6900 (1978).
[64] P. K. Gupta and J. C. Mauro, J. Chem. Phys. **130**, 094503 (2009).
[65] I. T. Penfold and P. S. Salmon, Phys. Rev. Lett. **67**, 97 (1991).
[66] J. D. Musgraves, P. Wachtel, S. Novak, J. Wilkinson, and K. Richardson, J. Appl. Phys. **110**, 063503 (2011).
[67] P. S. Salmon, A. Zeidler, and A. Polidori, "Data sets for Structure of As-Se glasses by neutron diffraction with isotope substitution," https://doi.org/10.15125/BATH-00902 (2020), University of Bath Research Data Archive.

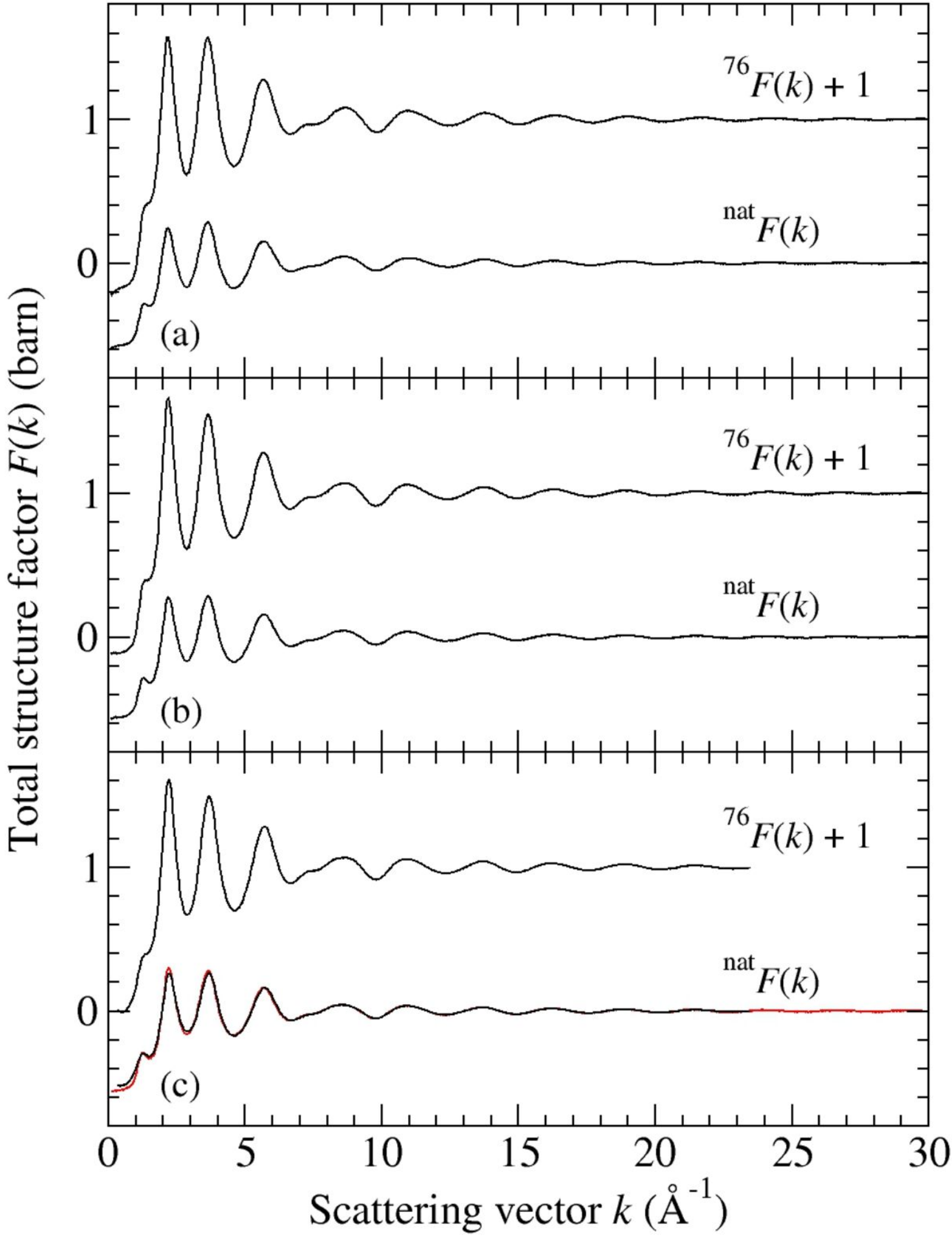
Total structure factor $F(k)$ (barn)
$^{76}F(k) + 1$
$^{nat}F(k)$
(a)
(b)
(c)
1
0
0
5
10
15
20
25
30
Scattering vector k (Å^{-1})

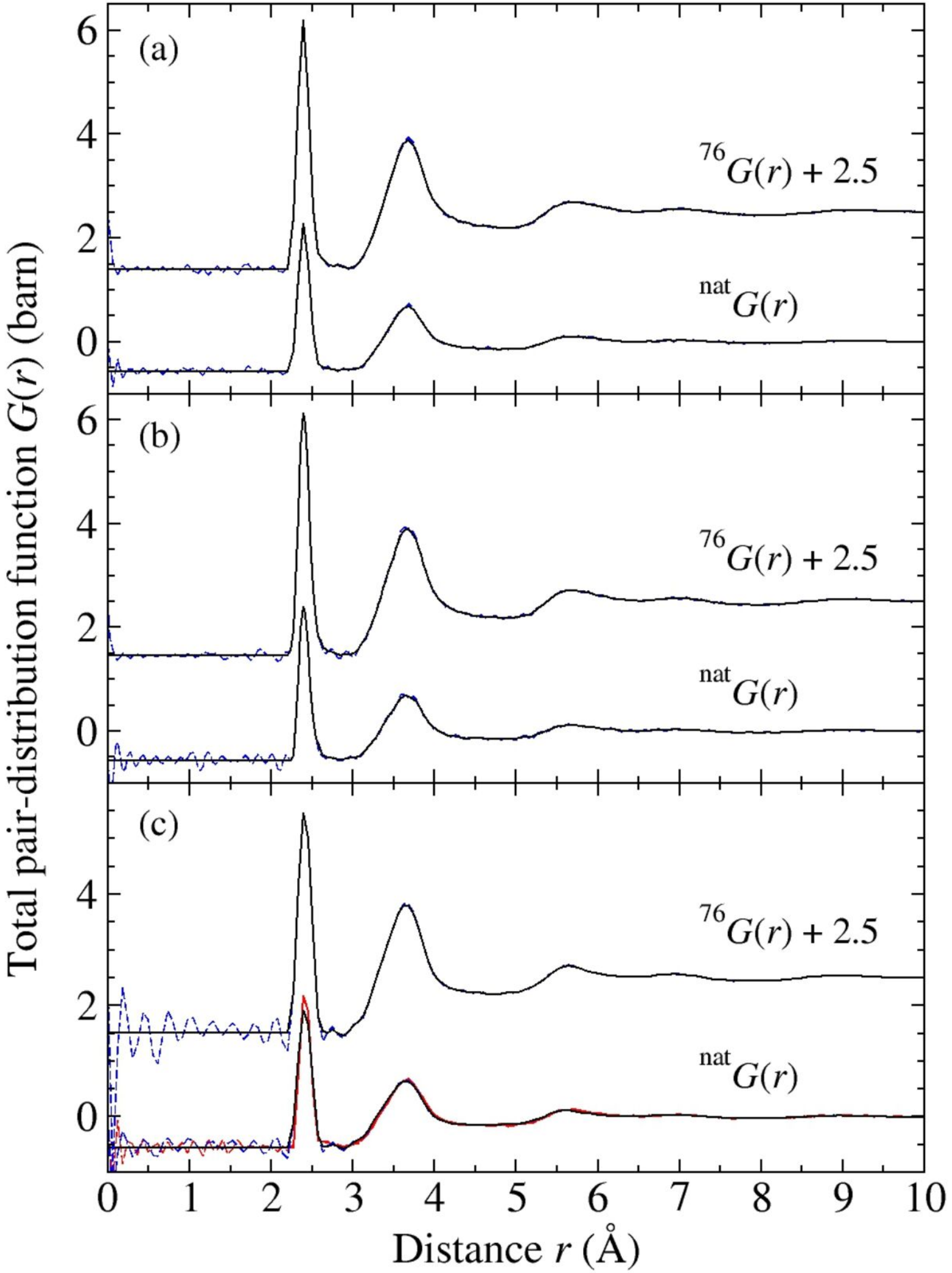
(a)
(b)
(c)
$^{76}G(r)$ + 2.5
$^{nat}G(r)$
Total pair-distribution function $G(r)$ (barn)
Distance r (Å)
0
1
2
3
4
5
6
7
8
9
10

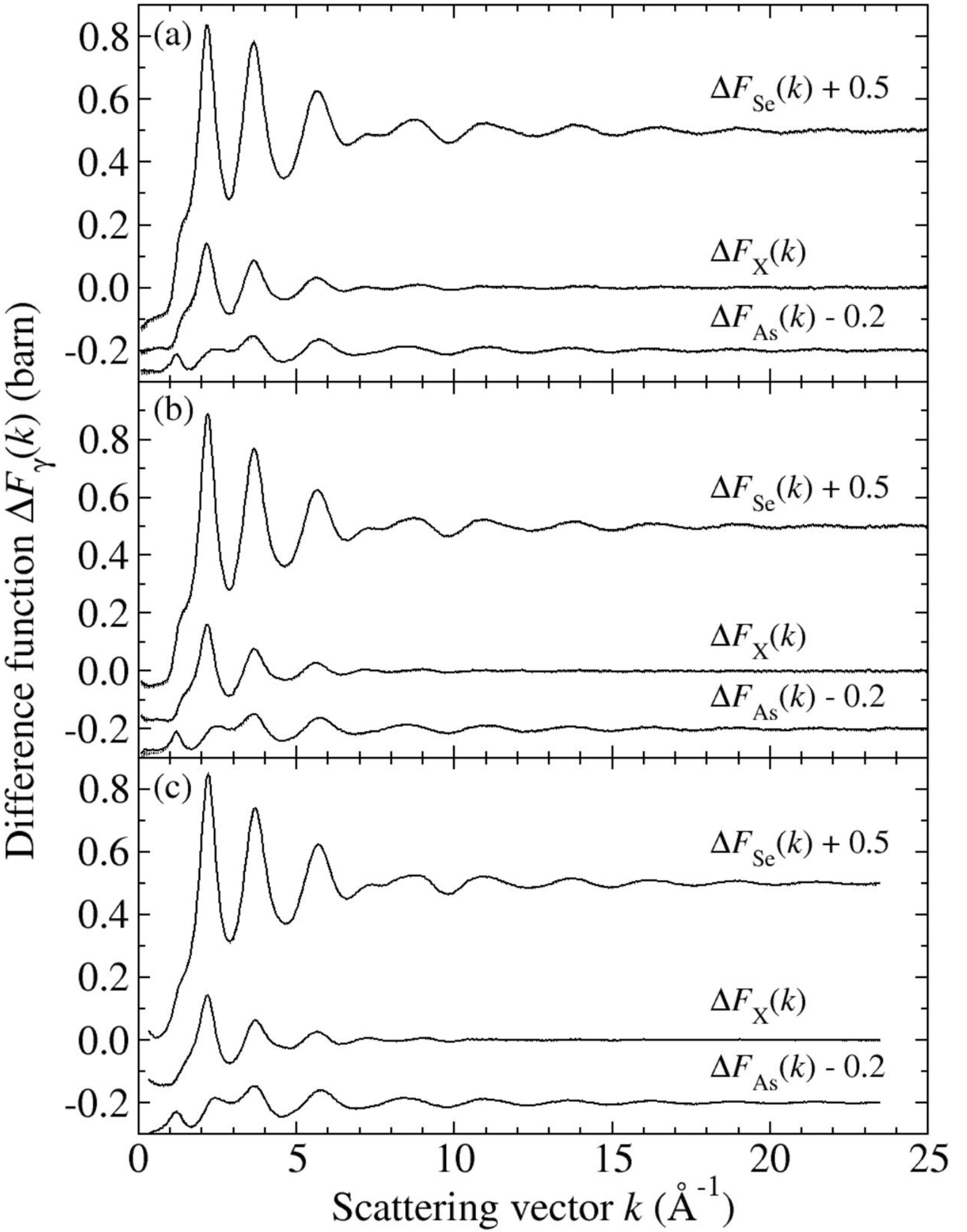
(a)
(b)
(c)
$\Delta F_{Se}(k) + 0.5$
$\Delta F_{X}(k)$
$\Delta F_{As}(k) - 0.2$
Difference function $\Delta F_{\gamma}(k)$ (barn)
Scattering vector k (Å^{-1})
0.8
0.6
0.4
0.2
0.0
-0.2
0
5
10
15
20
25

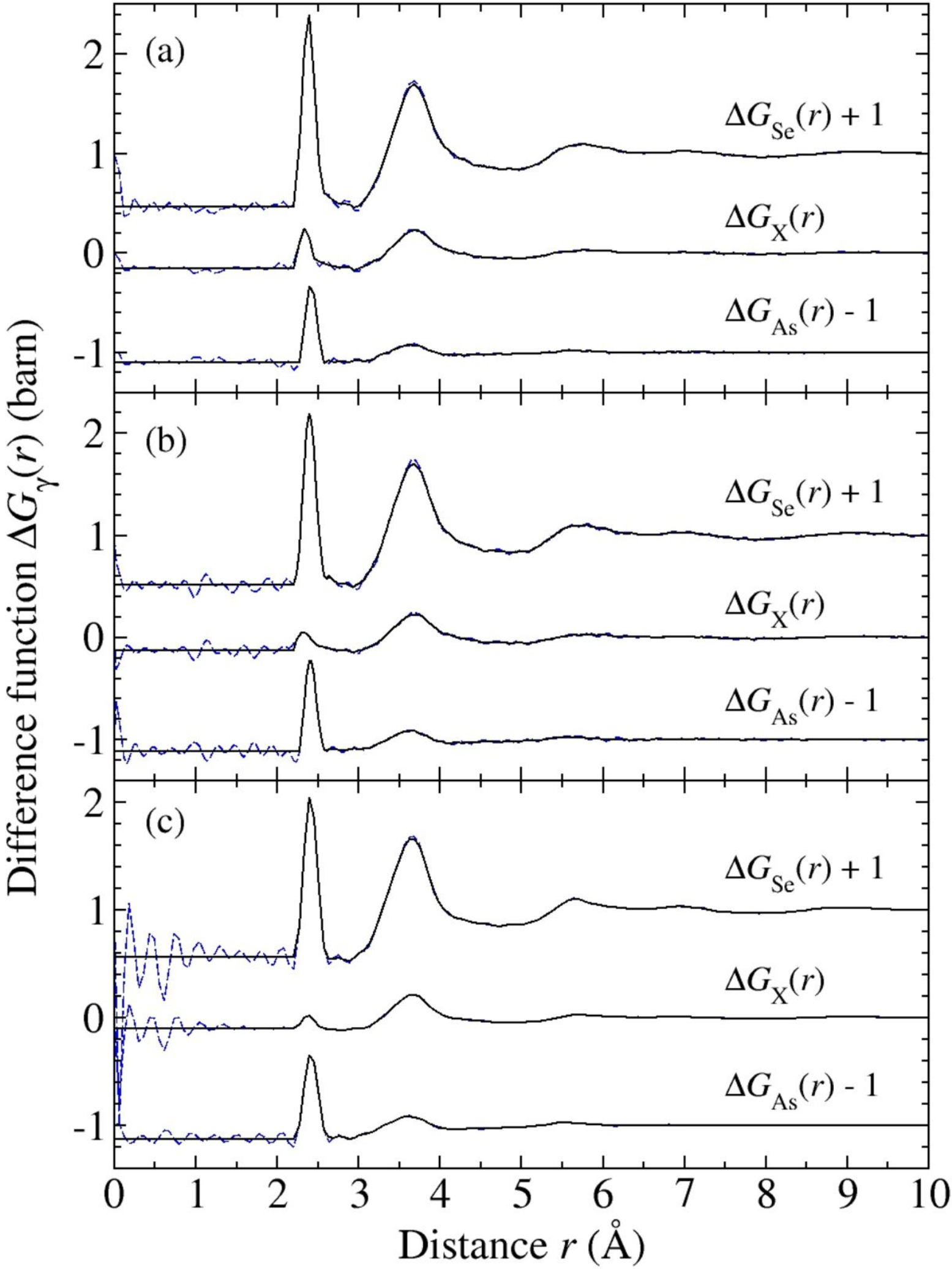
(a)
(b)
(c)
$\Delta G_{Se}(r) + 1$
$\Delta G_{X}(r)$
$\Delta G_{As}(r) - 1$
Difference function $\Delta G_{\gamma}(r)$ (barn)
Distance r (Å)
2
1
0
-1
0
1
2
3
4
5
6
7
8
9
10

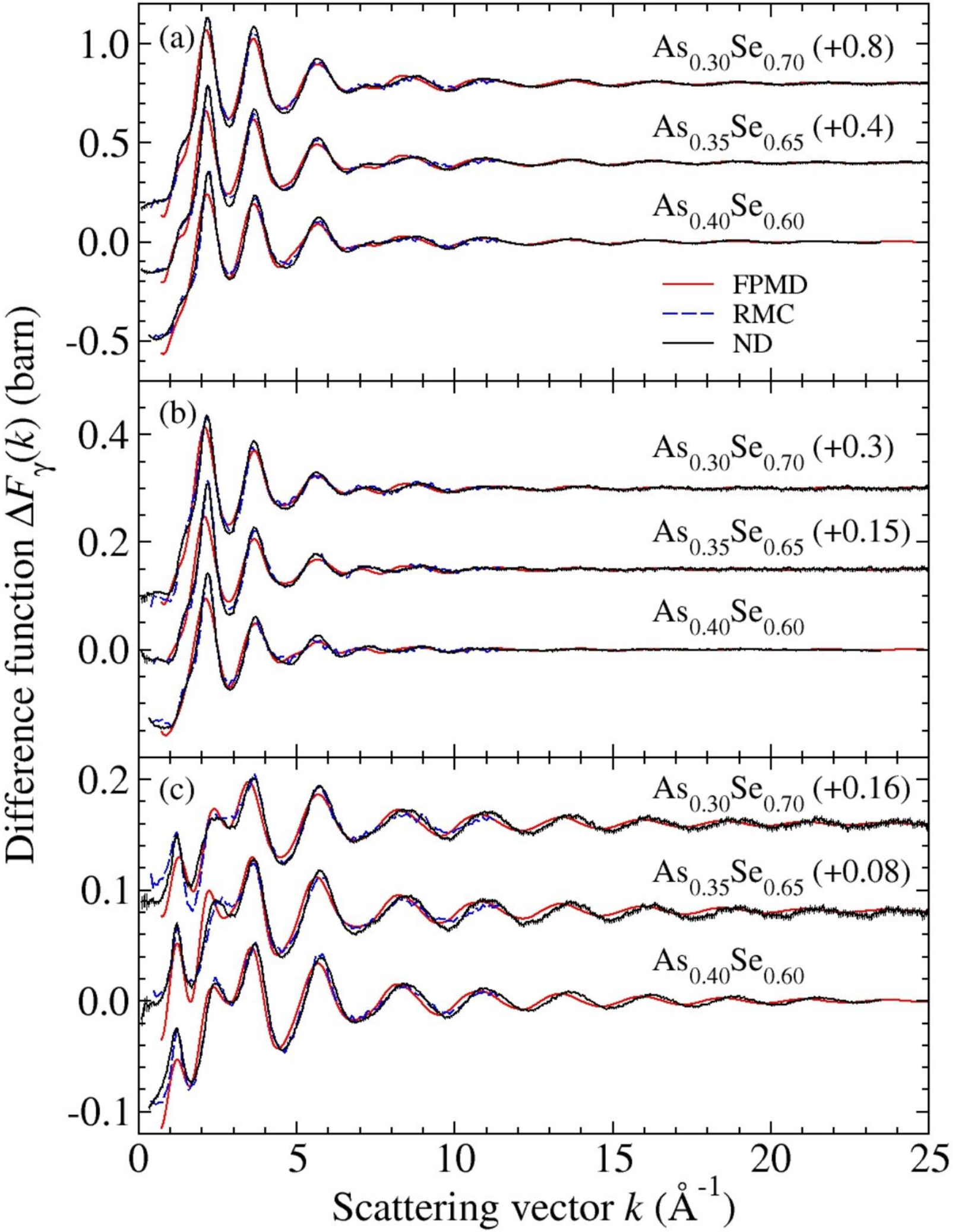
(a)
(b)
(c)
$As_{0.30}Se_{0.70}$ (+0.8)
$As_{0.35}Se_{0.65}$ (+0.4)
$As_{0.40}Se_{0.60}$
FPMD
RMC
ND
$As_{0.30}Se_{0.70}$ (+0.3)
$As_{0.35}Se_{0.65}$ (+0.15)
$As_{0.40}Se_{0.60}$
$As_{0.30}Se_{0.70}$ (+0.16)
$As_{0.35}Se_{0.65}$ (+0.08)
$As_{0.40}Se_{0.60}$
Difference function $\Delta F_\gamma(k)$ (barn)
Scattering vector k (Å^{-1})

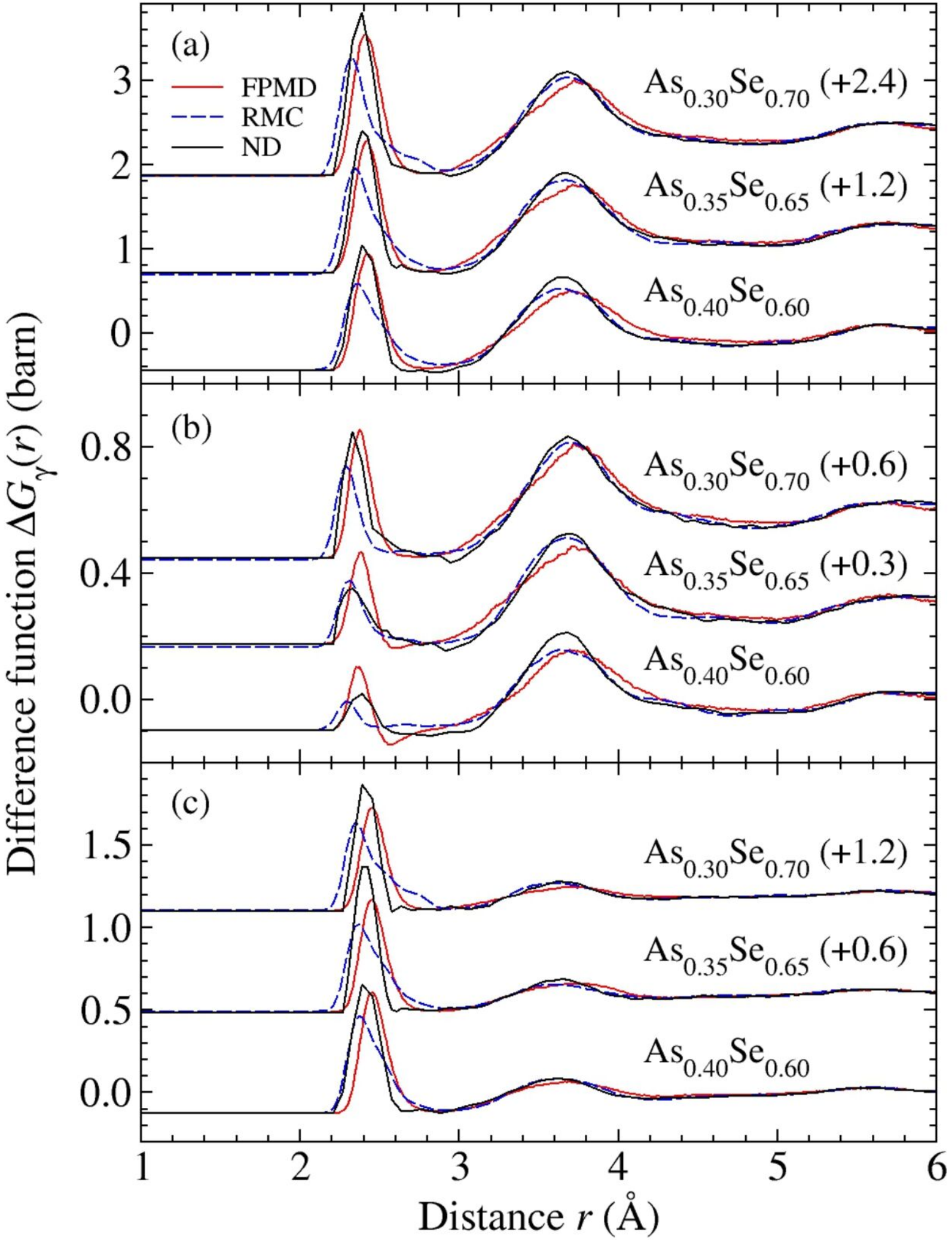
(a)
FPMD
RMC
ND
As0.30Se0.70 (+2.4)
As0.35Se0.65 (+1.2)
As0.40Se0.60
(b)
As0.30Se0.70 (+0.6)
As0.35Se0.65 (+0.3)
As0.40Se0.60
(c)
As0.30Se0.70 (+1.2)
As0.35Se0.65 (+0.6)
As0.40Se0.60
Difference function ΔGγ(r) (barn)
Distance r (Å)

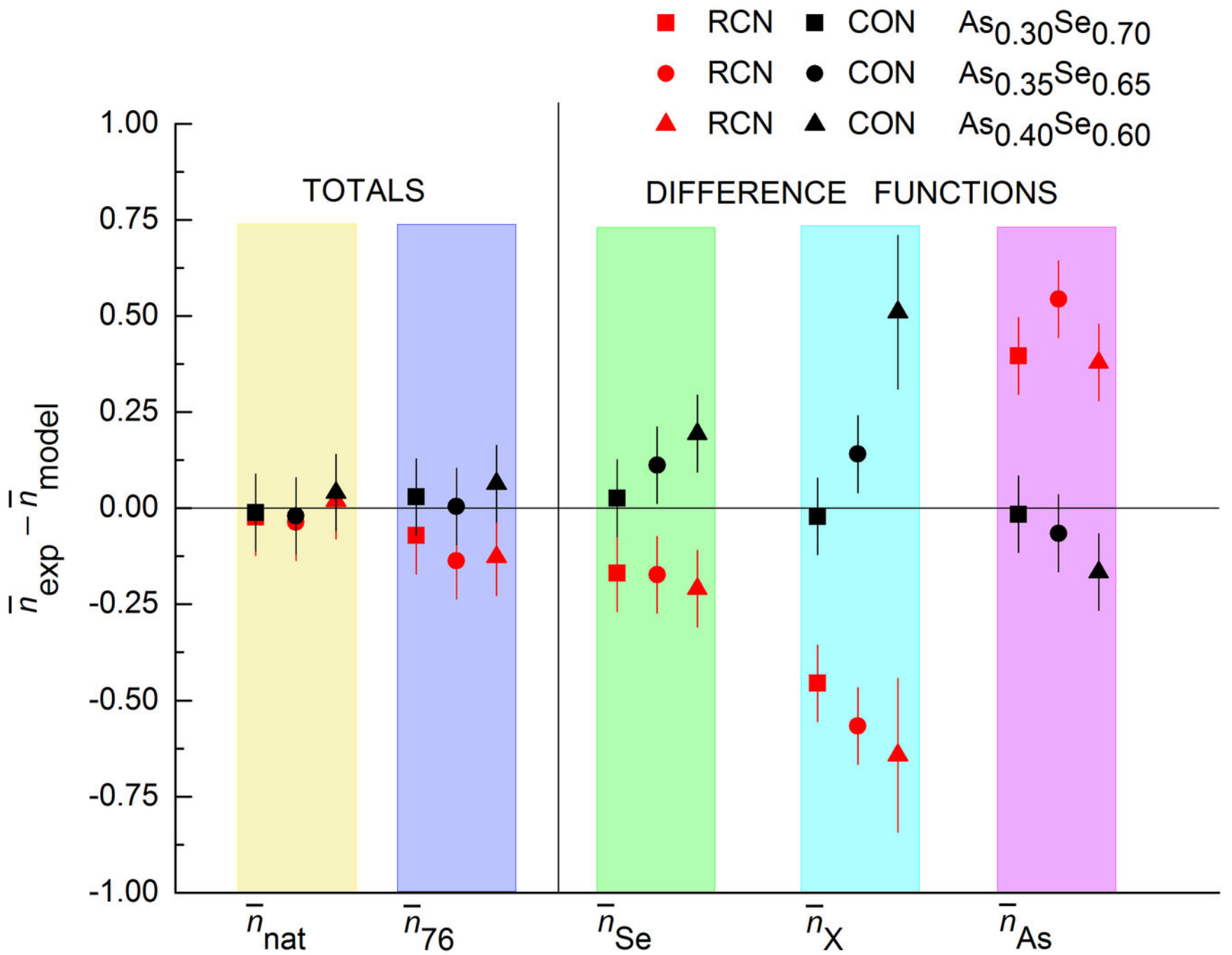
RCN CON As0.30Se0.70
RCN CON As0.35Se0.65
RCN CON As0.40Se0.60
TOTALS
DIFFERENCE FUNCTIONS
1.00
0.75
0.50
0.25
0.00
-0.25
-0.50
-0.75
-1.00
n̄exp − n̄model
n̄nat
n̄76
n̄Se
n̄X
n̄As